

This document is confidential and is proprietary to the American Chemical Society and its authors. Do not copy or disclose without written permission. If you have received this item in error, notify the sender and delete all copies.

Bovine Serum Albumin and Fibrinogen Adsorption at the 316L Stainless Steel/Aqueous Interface

Journal:	<i>The Journal of Physical Chemistry</i>
Manuscript ID	jp-2018-013473.R1
Manuscript Type:	Article
Date Submitted by the Author:	05-Apr-2018
Complete List of Authors:	Wood, Mary; University of Cambridge Department of Chemistry, Department of Chemistry Payagalage, Charanee; University of Cambridge Department of Chemistry, Department of Chemistry Geue, Thomas; Paul Scherrer Institut, LNS

SCHOLARONE™
Manuscripts

1
2
3 **Bovine Serum Albumin and Fibrinogen Adsorption at the 316L Stainless Steel/Aqueous**
4
5 **Interface**
6

7 Mary H. Wood,^{1*} Charanee Galabada Payagalage,¹ Thomas Geue²
8

9 ¹*Department of Chemistry, University of Cambridge, Lensfield Road, Cambridge, CB2 1EW,*
10

11 *UK*
12

13 ²*Laboratory of Neutron Scattering and Imaging, Paul Scherrer Institute, 5232 Villigen PSI,*
14

15 *Switzerland*
16

17 **maryhwood@gmail.com (+44)1214 142966*
18
19
20
21
22
23
24
25
26
27
28
29
30
31
32
33
34
35
36
37
38
39
40
41
42
43
44
45
46
47
48
49
50
51
52
53
54
55
56
57
58
59
60

1
2
3 **ABSTRACT:** The binding of bovine serum albumin (BSA) to a 316L stainless steel surface from
4 a buffer solution has been characterized using neutron reflectometry (NR) and quartz crystal
5 microbalance (QCM) measurements; coverage at all concentrations up to a near-
6 physiological concentration was found to be relatively low (< 20 %); the protein followed a
7 two-step isotherm adsorption model type and the overall thickness at the higher
8 concentrations (around 80 Å) suggested possible multi-layering and/or protein unfolding. As
9 it has been postulated that BSA may inhibit the further adsorption of another blood plasma
10 protein—fibrinogen—the effects of pre-adsorbing BSA on fibrinogen adsorption were
11 examined, first by prior physisorption of BSA to the stainless steel surface and second by
12 pre-treating the stainless steel with a layer of SDS to render it more hydrophobic. While the
13 pre-adsorption of BSA to an untreated stainless steel surface did slightly decrease the
14 amount of fibrinogen adsorbed initially, it had no inhibiting effect if a solution containing
15 solely fibrinogen subsequently flowed through. In contrast, the SDS-treated surface yielded
16 both an increased BSA adsorption and consistently decreased fibrinogen adsorption.
17
18
19
20
21
22
23
24
25
26
27
28
29
30
31
32
33
34
35
36
37
38
39
40
41
42
43
44
45
46
47
48
49
50
51
52
53
54
55
56
57
58
59
60

INTRODUCTION

Understanding the interaction of potential biomaterials with physiological proteins is extremely important when considering their biocompatibility. One of the most persisting concerns when introducing a new material into the body is the possible onset of thrombosis, whereby uncontrollable clotting at the surface results in large emboli that may break away and block blood veins with potentially fatal consequences. The formation of blood clots via coagulation is an extremely complex process and is considered to follow two possible pathways—the extrinsic pathway, which is initiated when trigger chemicals are released from damaged blood vessel walls, and the intrinsic pathway, which is initiated by platelet damage or by contact of the blood with a foreign body such as a biomaterial. Traditionally, it has been thought that the extrinsic pathway plays no role in coagulation resulting from biomaterial introduction, although recent studies have shed some doubt on this view¹. The exact mechanisms of biomaterial-induced coagulation are not yet completely understood and appear to rely on a great number of factors. However, it is well-established that any surface will be coated in a layer of proteins within seconds of encountering the blood plasma, and that this adsorbed protein layer will be critical in determining ensuing success or rejection of the biomaterial².

As fibrinogen plays a direct role in the coagulation process, it is unsurprising that its interaction with biomaterials has been of particular interest, and indeed platelet adhesion to the biomaterial has been found to be dependent both on amount of fibrinogen adsorbed and, crucially, on its adsorbed state conformation, which is dependent on the surface characteristics of the biomaterial^{1,3-5}. Whilst fibrinogen is not the most abundant protein in the blood plasma, it is often the most extensively adsorbed across a range of surface types

1
2
3 (although the Vroman effect may subsequently diminish its surface presence)⁶⁻⁸ ; hence, a
4
5 surface that may be considered 'invisible' to the fibrinogen protein has long been sought.
6
7 One commonly-used strategy is to pre-treat the biomaterial surface with serum albumin.
8
9 This is the most abundant blood plasma protein and is not involved in the coagulation
10
11 process, its function being rather the transport of fatty acids and other species⁹. Pre-
12
13 adsorption of albumin is thought to prevent subsequent adsorption of coagulation proteins
14
15 such as fibrinogen and hence to render the surface more biocompatible¹⁰⁻¹². As albumin
16
17 only binds weakly to most surfaces, particularly when in competition with other plasma
18
19 proteins, it is necessary to pre-bind the albumin before exposure to physiological fluids^{11,13}.
20
21 Indeed, some studies have found that it is only significantly effective if the physisorption is
22
23 enhanced by making the surface more hydrophobic, or if the albumin is cross-linked itself
24
25 when adsorbed^{14,15}. One disadvantage of the albumin pre-treatment is that adsorbed
26
27 proteins tend to denature over time or to desorb; as many implants need to remain in the
28
29 body safely for a long duration, a surface treatment that will endure over a long timescale is
30
31 crucial¹⁰. Increasing the hydrophobicity of the surface has been found to improve the
32
33 longevity of albumin-coated devices; this effect is presumed to arise both from an increase
34
35 in the amount adsorbed, and also from the increased unfolding and relaxation of the
36
37 albumin protein molecules, such that their hydrophobic domains are able to interact with
38
39 the surface, leading to an overall increased surface footprint¹⁶⁻¹⁹. Uyen *et al.* observed that
40
41 islands of albumin that adsorb initially onto hydrophobic surfaces grow more over time than
42
43 on hydrophilic surfaces; they related this to increased lateral interactions between the
44
45 adsorbed albumin molecules²⁰. In addition, it has been shown that BSA adsorption to
46
47 various grades of stainless steel, including the 316L surgical grade used in this study, is liable
48
49 to induce significant release of metal ions into solution²¹. As the corrosion of biomedical
50
51
52
53
54
55
56
57
58
59
60

implants is extremely detrimental to their usability, surface modification to protect the stainless steel over a long period of implantation is clearly advisable.

In this work, the adsorption of bovine serum albumin (BSA) on a 316L stainless steel surface was measured and its effect on further adsorption of fibrinogen monitored using both neutron reflectometry (NR) and quartz crystal microbalance (QCM). NR was also used to assess the efficacy of pre-coating the stainless steel surface with sodium dodecyl sulfate (SDS)—in an attempt to render it more hydrophobic—on both improving BSA adsorption and hindering fibrinogen adsorption. NR is a powerful technique for monitoring the structure of buried interfacial layers, particularly for organic species that are harder to detect using X-rays²². Full details of the underlying theory for the technique may be found elsewhere^{23,24}. The NR data are modelled to give a profile of the scattering length density (SLD) as a function of the distance along the surface normal, z . SLD values of the materials of interest in this work are given in Table 1. We have previously demonstrated that by using an electron-beam deposition technique, a film of stainless steel can be successfully deposited onto a silicon substrate to provide a model stainless steel surface that is suitable for NR experiments²⁵. Here, we extend the technique to a more complex protein system. In addition, QCM allows measurement of protein adsorption at the solid/liquid interface in real time via changes in the frequencies of a resonant crystal beneath the stainless steel layer²⁶.

Table 1. SLD Values. 'BSA' = bovine serum albumin. The SLD of the protein is dependent on the solvent contrast, due to its large number of exchangeable protons.

	SLD / $\times 10^{-6} \text{ \AA}^{-2}$		SLD / $\times 10^{-6} \text{ \AA}^{-2}$
Si	2.072	Fe ₂ O ₃	7.176
SiO ₂	3.484	Cr ₂ O ₃	5.106
Fe	8.020	H ₂ O	-0.561
Cr	3.027	D ₂ O	6.335
Ni	9.406	BSA / 100% H ₂ O	1.853
Mn	-3.054	BSA / 100 %	3.056
		D ₂ O	

EXPERIMENTAL

Materials. For the NR experiments, 316L stainless steel films (10–20 nm thickness) were deposited onto polished silicon substrates, (111)-orientation, (n)-type, using electron-beam deposition *in vacuo* at the Nanoscience Centre at the University of Cambridge. 316 stainless steel QCM sensors were purchased from Q-sense. Fibrinogen and Bovine serum albumin were purchased from MP Biomedicals and all other chemicals were acquired from Sigma-Aldrich (all with purities > 99 %). All experiments were conducted in phosphate buffered saline ('PBS', 0.01 M, pH 7.4).

XRR. XRR profiles were collected at the Cavendish Laboratory, Cambridge using a Bruker D8 X-ray diffractometer with copper target and a Goebel mirror. An accelerating voltage of 50 kV was used and a primary beam size of 0.1 mm. 0.35 mm Soller slits were inserted before the detector, which was operated in 1D mode. XRR data were fitted using GenX 2.0.0 software²⁷.

NR. Neutron reflectometry data were collected using the AMOR instrument at the Paul Scherrer Institute in Switzerland. Full details of the instrument may be found elsewhere²⁸. The instrument was used in non-polarised mode; stainless steel-coated silicon blocks (55 mm diameter, 5 mm thick) were mounted in a custom-made aluminium cell with a PTFE trough. The bare substrates were characterised in D₂O and H₂O prior to introduction of the protein solutions. Sample 2 was pre-coated with an SDS layer by soaking in an SDS/ethanol solution (7 mM) for 24 hours before rinsing and drying under N₂ prior to mounting in the sample cell. NR data were fitted using the RasCAL software²⁹.

1
2
3 **QCM.** The 316 stainless steel sensors were cleaned prior to use in 1% Hellmanex II
4
5 (30 min), rinsed with ultrapure water (18 M Ω cm) and dried with N₂; they were then
6
7 sonicated in 99% ethanol (10 min), and rinsed and dried again before cleaning by UV/ozone
8
9 (10 min). Experiments were conducted on a Q-sense E4 QCM at the Nanoscience Centre,
10
11 University of Cambridge. The QCM instrument was cleaned with 2% Hellmanex and rinsed
12
13 thoroughly with ultrapure water before loading of the sensors. Background solution (PBS)
14
15 was flowed through and the sensors left for 24 h to equilibrate. Fresh electrolyte was then
16
17 flowed through until the frequencies had stabilized. The sample solutions were then
18
19 introduced to each sensor (flow rate 0.15 mL min⁻¹) until the frequencies were stable. After
20
21 the systems had reached equilibrium, background electrolyte was reintroduced to each one
22
23 until no further changes were observed. Data were analyzed using the QSense Dfind 1.0
24
25 software. For Sauerbrey model fits, the f₃ overtone was used; for viscoelastic model fits, a
26
27 Voigt model was used.
28
29
30
31
32
33
34

35 **RESULTS AND DISCUSSION**

36
37
38 **NR.**

39
40 *Sample 1.*
41
42
43
44
45
46
47
48
49
50
51
52
53
54
55
56
57
58
59
60

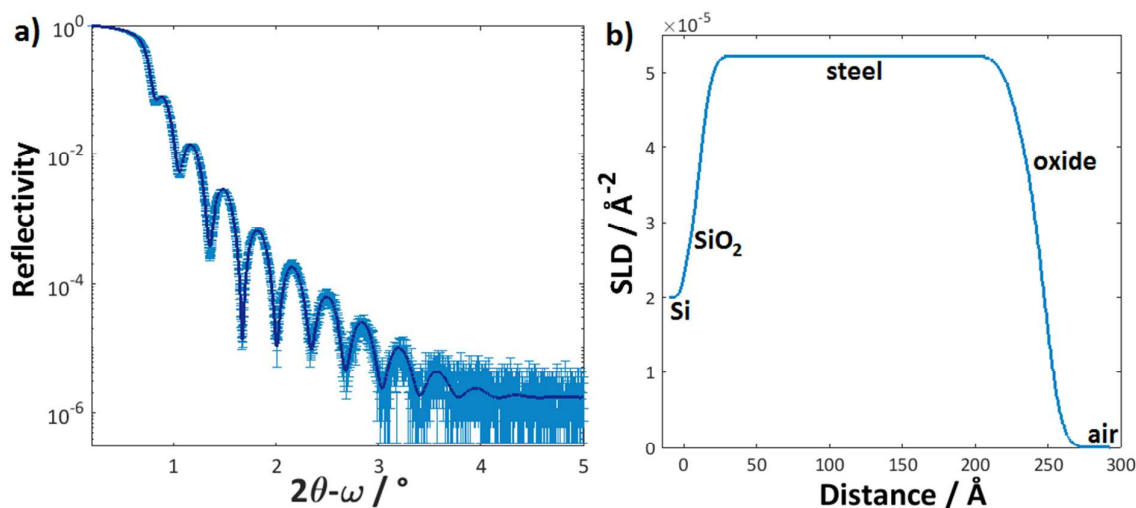


Figure 1a) XRR data (points) and model fits (solid lines) for a stainless steel film on a silicon substrate (Sample 1). b) Corresponding SLD profiles for the model fit.

Sample 1 was characterized using XRR prior to analysis by NR; the data and model fits are shown in Figure 1. The data were fitted with just one metal layer for the stainless steel of thickness 217 \AA ($\pm 2 \text{ \AA}$) and an oxide layer of thickness 21 \AA ($\pm 2 \text{ \AA}$), in good agreement with the estimated deposition thickness values. (Error margins taken from limits of reasonable fit.)

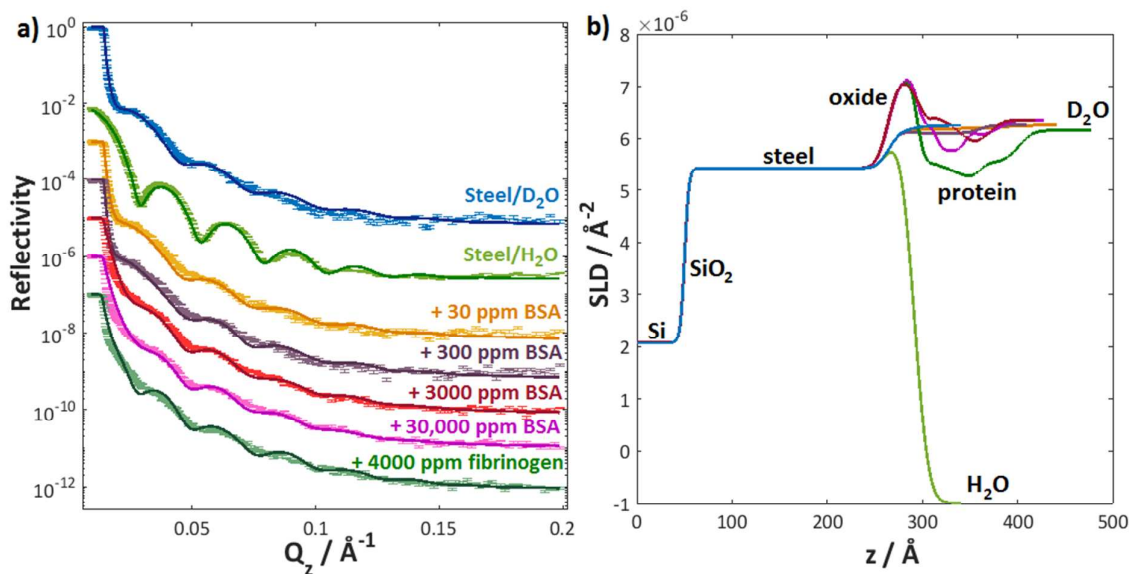


Figure 2a) Neutron reflectometry data (points) and model fits (solid lines) for sample 1, showing the untreated stainless steel surface under D_2O and H_2O and with increasing concentrations of protein added, as labelled. (D_2O and H_2O are given as shorthand for PBS/ D_2O and PBS/ H_2O). Data offset vertically for clarity. Only D_2O data are shown for the protein solutions as these show the greatest contrast. b) Corresponding SLD profiles for the model fits.

The NR data and model fits for the untreated stainless steel sample are shown in Figure 2; the stainless steel film under PBS/water could be modelled with a metal layer of thickness 214 \AA ($\pm 2 \text{ \AA}$), roughness 15 \AA and SLD $5.42 \times 10^{-6} \text{ \AA}^{-2}$, and an oxide layer of thickness 30 \AA ($\pm 3 \text{ \AA}$) and SLD $6.15 \times 10^{-6} \text{ \AA}^{-2}$. The thicknesses are in good agreement with the XRR data (the increase in oxide thickness is attributed to the UV/ozone cleaning prior to NR measurements) and the SLD values are similar to those seen previously²⁵, with the oxide SLD consistent with that expected for a mixture of iron and chromium oxides (values for pure Cr_2O_3 and Fe_2O_3 would be 5.11 and $7.17 \times 10^{-6} \text{ \AA}^{-2}$, respectively). While the SLD of 316L stainless steel should theoretically be closer to $7 \times 10^{-6} \text{ \AA}^{-2}$, an increased amount of Mn

(which has a very low SLD) was previously observed in the deposited films, hence decreasing the overall SLD²⁵.

Table 2. Adsorbed Amounts Calculated from Neutron Fits for Both Samples

Error margins are calculated from the maximum and minimum acceptable fits to the NR data. *Surfaces finally washed with PBS (no protein) following adsorption.

	[BSA] / ppm	[fibrinogen] / ppm	Amount adsorbed /mg m ⁻²
Sample 1	30	0	0.25 (\pm 0.2)
	300	0	0.58 (\pm 0.4)
	3000	0	0.74 (\pm 0.4)
	30000	0	1.22 (\pm 0.4)
	30000	4000	3.35 (\pm 0.4)
	0	4000	4.75 (\pm 0.4)
	0*	0*	3.53 (\pm 0.4)
Sample 2 (pre-treated with SDS)	30000	0	1.77 (\pm 0.4)
	30000	4000	2.29 (\pm 0.4)
	0	4000	3.64 (\pm 0.4)
	0*	0*	2.90 (\pm 0.4)

Only very slight changes in the measured data were seen after the addition of 30 ppm and 300 ppm BSA; these could be simply modelled by inclusion of a Gaussian protein layer. For the 3000 and 30,000 ppm BSA, a Gaussian layer was unable to satisfactorily fit the data; instead, a block model with several layers was used, where the % of hydration (i.e. extent of solvent inclusion in the protein layer) was allowed to vary for each layer. The overall protein thicknesses for 3000 and 30,000 ppm were 75 Å and 83 Å respectively. Using either the area under the Gaussian curve or the area encapsulated by the block models as appropriate, the amount of protein adsorbed per square metre of the substrate was calculated and used to infer an adsorption isotherm for BSA on a 316L stainless steel surface, shown in Figure 3 (x-axis plotted as a log scale for clarity). The fitted amounts adsorbed are given in Table 2.

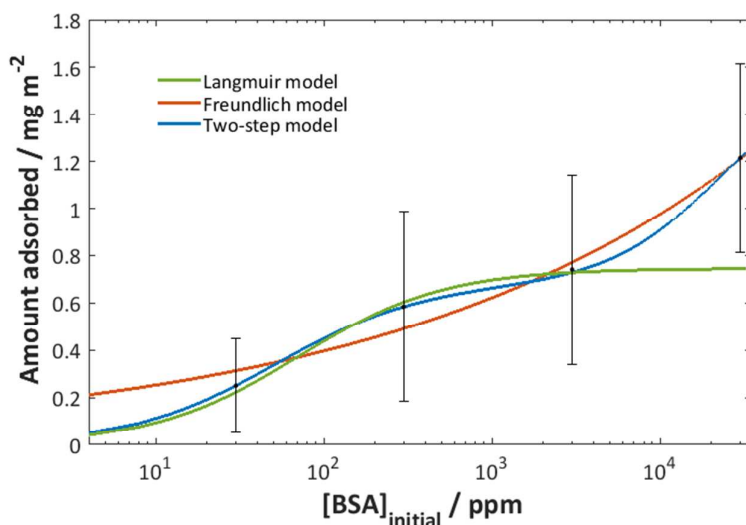


Figure 3. Isotherm calculated from the fitted neutron reflectometry data for increasing concentrations of BSA on the untreated stainless steel surface. Data are plotted as points with model fits as solid lines, as labelled. Error margins are calculated from the limits of a reasonable fit to the neutron data.

Up to and including 3000 ppm BSA, a simple Langmuir model was sufficient to fit the data; however, the data point at 30,000 ppm did not fit this trend. Two alternative isotherm models were fitted to the data, as shown in Figure 3. The Freundlich isotherm model gave an more acceptable fit to the data; this model assumes ongoing interaction between the adsorbed protein and incoming protein molecules, given by the equation:

$$v = v_{max} K_F c^{\frac{1}{n}}$$

where v is the fraction adsorbed, v_{max} is the final plateau of adsorption, K_F is the affinity parameter, c is the adsorbate concentration and n is a dimensionless constant > 1 that relates to the strength of adsorbate interactions with either the substrate or other adsorbate molecules^{30,31}. This would not be an unreasonable assumption for protein adsorption, since proteins are known to change in structure upon adsorption to solid

1
2
3 surfaces, and the large number of functional groups on any protein makes interaction with
4
5 other adsorbing proteins feasible.
6

7
8 The two-step isotherm model was proposed by Zhu *et al.* and assumes Langmuir-like
9
10 behavior at low concentrations, but with a second plateau at higher concentrations; they
11
12 found this model described systems in which monomer adsorption at low concentrations
13
14 was followed by adsorption of aggregated molecules at higher concentrations³². It has also
15
16 been used previously to describe protein adsorption due to the potential protein-protein
17
18 interactions in the adsorbed layers²⁵. The isotherm model is given by:
19
20

$$21 \quad v = \frac{v_{max} K_1 c \left(\frac{1}{n} + K_2 c^{n-1} \right)}{1 + K_1 c (1 + K_2 c^{n-1})}$$

22
23
24
25 where K_1 and K_2 are affinity parameters for the first and second steps respectively. As shown
26
27 in Figure 3, the two-step model gives the best fit to the isotherm data; however, this might
28
29 be expected for the greater number of parameters that can be fitted, particularly given the
30
31 relatively large error bars associated with these measurements.
32
33

34
35 Both the Freundlich and two-step isotherm models give acceptable fits to the
36
37 experimental data, indicating that at higher protein concentrations some kind of interaction
38
39 with the protein already adsorbed may lead to increased adsorption, possibly in the form of
40
41 a bilayer; this would agree well with the increased layer thicknesses seen at higher
42
43 concentrations (as shown in the SLD profile in Figure 2b) of 75 and 83 Å at 3,000 and 30,000
44
45 ppm. The dimensions of a hydrated bovine serum albumin molecule have been estimated³³
46
47 as 140 Å x 40 Å x 40 Å; a bilayer in which the larger dimension is lying parallel to the surface
48
49 would, therefore, be consistent with the fitted data for the higher protein concentrations,
50
51 and accord well with the fitted isotherm models. Similar multi-step behavior has been
52
53 previously observed for albumin at the stainless steel/buffer solution interface and ascribed
54
55
56
57
58
59
60

1
2
3 to various protein-protein interactions within the adsorbed film, although further more
4
5 specific measurements would be necessary to confirm this^{34,35}.
6

7
8 Assuming a volume per molecule of BSA³⁶ of around $1.08 \times 10^5 \text{ \AA}^2$, and treating the
9
10 protein molecules as spheres, each molecule might be expected to occupy approximately
11
12 5500 \AA^2 on the stainless steel surface. The areas per molecule calculated from the values in
13
14 Table 2 would yield an area per molecule of 15000 \AA^2 at 3000 ppm and 9000 \AA^2 at 30,000
15
16 ppm. This is in good agreement with the low surface coverage suggested by the model fit to
17
18 the neutron data, where a large amount of water inclusion was necessary for each layer (\geq
19
20 80 %).
21
22

23
24 The adsorbed amount for the BSA/316L stainless steel system across this
25
26 concentration range is significantly lower than that seen for an isotherm of fibrinogen
27
28 previously derived from NR data²⁵. (This trend is also observed when both isotherms are
29
30 plotted in terms of molar concentration, as demonstrated in Figure S1.) The Langmuir
31
32 plateau value seen here is very similar to that observed previously for BSA adsorbed onto
33
34 316L stainless steel particles for comparable protein concentrations around pH 7^{37,38}. A
35
36 higher adsorption coverage was seen by Van Enkevort *et al.* for a 304 stainless steel slide
37
38 measured using ^{125}I -labelled albumin³⁹; however, use of isotopic labelling is known to lead
39
40 to overestimation of adsorption coverages, due to free ^{125}I that remains associated with the
41
42 surface^{34,40}. The slight differences in grade of stainless steel may also account for differences
43
44 in the protein surface coverage, particularly since stainless steel particles are known to be
45
46 enriched in manganese, similarly to the deposited films used here⁴¹.
47
48
49

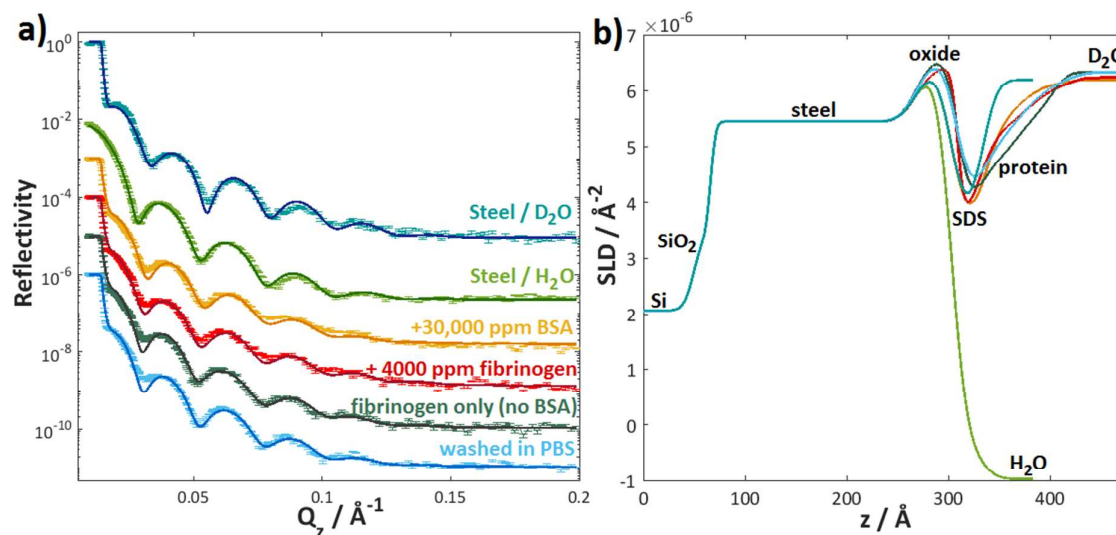
50
51 When a solution of 30,000 ppm BSA plus 4000 ppm fibrinogen was subsequently
52
53 flushed through the cell, the overall amount of protein adsorbed increased to 3.0 mg m^{-2} (\pm
54
55 0.4 mg m^{-2}). This is less than the amount adsorbed calculated from NR data for fibrinogen
56
57

1
2
3 on its own on a 316L stainless steel surface observed previously—4.7 mg m⁻² at 4000 ppm
4
5 fibrinogen²⁵. Even within the relatively large error bars of the experiment, this reflects a
6
7 significant enough decrease to indicate that the adsorbed BSA does prevent fibrinogen
8
9 adsorption to some extent. However, when the cell was flushed through with a solution of
10
11 fibrinogen alone (4000 ppm), the adsorbed amount increased to 4.75 mg m⁻² (\pm 0.4 mg m⁻²).
12
13
14 This almost exactly matches the value seen previously when fibrinogen was allowed to
15
16 adsorb on stainless steel that had not previously encountered BSA. It would therefore seem
17
18 that the BSA only has a preventative effect on the fibrinogen adsorption if it remains the
19
20 dominant species in the bulk solution, and is presumably quickly displaced from the surface
21
22 by the fibrinogen.
23
24

25
26 Wertz *et al.* put forward the interesting theory that the adsorption of albumin is
27
28 greatly dependent on the rate at which it arrives at the surface—they posit that when the
29
30 rate is slow, small amounts of albumin that arrive initially and adsorb in their molecular
31
32 form will unfold and spread across the entire surface, preventing further adsorption,
33
34 whereas rapidly-arriving albumin (i.e. from high initial bulk concentrations) will adsorb in
35
36 larger amounts as there is no time for this unfolding⁴². However, the results shown here
37
38 would seem to contradict this theory, at least to some extent, as the increasing
39
40 concentrations of albumin were flowed over the same sample without rinsing in between,
41
42 and as each measurement took in excess of 6 hours to complete, there should have been
43
44 ample time for such unfolding—however, there does not seem to be any inhibition of
45
46 further albumin adsorption at the higher concentrations, which suggests that the protein
47
48 adsorbed at lower concentrations has not altered the surface significantly enough to
49
50 prevent further adsorption. These contrasting observations to those of Wertz *et al.* may
51
52 arise from the differences in surface type, as their measurements were conducted on a
53
54
55
56
57

1
2
3 hydrophobic, C16 self-assembled monolayer surface, whereas the negatively-charged
4
5 stainless steel sample used in this work may be less conducive to protein unfolding, given
6
7 that the albumin molecules are also expected to be negatively-charged at this pH²¹. This
8
9 further highlights the importance of surface preparation with respect to biomaterial design.
10

11
12 *Sample 2.* In an attempt to increase the BSA coverage, and therefore decrease
13
14 fibrinogen adsorption, a second stainless steel sample was pre-treated with an SDS/ethanol
15
16 solution in the hope of pre-adsorbing a layer of SDS and hence rendering the surface more
17
18 hydrophobic. The data and model fits are shown in Figure 4; similarly to sample 1, a
19
20 stainless steel layer 211 Å thick (± 3 Å) with SLD $5.5 \times 10^{-6} \text{ Å}^{-2}$ and roughness 15 Å and an
21
22 oxide layer 25 Å thick (± 3 Å) with SLD $7.1 \times 10^{-6} \text{ Å}^{-2}$ were found to give a good fit to the data.
23
24 In addition, an SDS layer (SLD $0.34 \times 10^{-6} \text{ Å}^{-2}$) 30 Å (± 3 Å) thick was found to have adsorbed
25
26 with 46% coverage (as seen by the significant dip in the SLD profile adjacent to the stainless
27
28 steel surface in Figure 4b). This demonstrated that the pre-soaking of the stainless steel
29
30 steel surface in Figure 4b). This demonstrated that the pre-soaking of the stainless steel
31
32 substrate in the SDS/ethanol solution had been successful in yielding a surface layer about
33
34 half of that expected for a fully well packed surfactant layer.
35
36



1
2
3 **Figure 4a) Neutron reflectometry data (points) and model fits (solid lines) for sample 2,**
4 **showing the untreated stainless steel surface under D₂O and H₂O and with increasing**
5 **concentrations of protein added, as labelled. Data offset vertically for clarity. Only D₂O**
6 **data are shown for the protein solutions as these show the greatest contrast. b)**

7
8
9
10
11
12 **Corresponding SLD profiles for the model fits.**
13

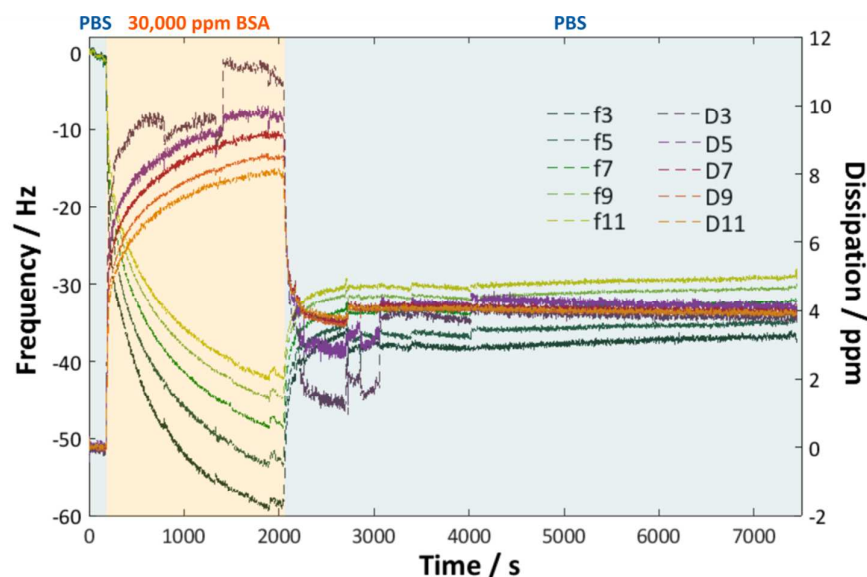
14
15 Upon addition of BSA, a Gaussian model was again used to fit the adsorbed layer,
16 with calculated amounts adsorbed summarized in Table 2. At a concentration of 30,000 ppm
17 BSA, an increase in the amount of protein adsorbed in comparison to Sample 1 was
18 observed, suggesting the SDS did indeed facilitate BSA adsorption. Significantly lower
19 amounts of adsorbed protein in comparison to Sample 1 were seen upon subsequent
20 addition of fibrinogen, both with BSA and by itself. When 4000 ppm fibrinogen was flushed
21 through the cell, the amount adsorbed was 3.64 mg m^{-2} ($\pm 0.4 \text{ mg m}^{-2}$), which is
22 considerably less than that seen for fibrinogen on the bare stainless steel substrate²⁵. While
23 the different proteins cannot be distinguished from this data as both were in protonated
24 form with similar SLD values ($3.06 \times 10^{-6} \text{ \AA}^{-2}$ for BSA and $3.26 \times 10^{-6} \text{ \AA}^{-2}$ for fibrinogen in 100
25 % D₂O), the natural conclusion is that the presence of the SDS is ensuring more BSA is
26 retained on the surface with a subsequent inhibitory effect on fibrinogen adsorption. High
27 concentrations of SDS have previously been thought to have a partially denaturing effect on
28 albumin pre-adsorbed onto 316L stainless steel surfaces⁴³. It is possible that the strength of
29 the SDS-albumin interaction may also be causing some unfolding in this case, which may
30 contribute to the prevention of fibrinogen adsorption.
31
32
33
34
35
36
37
38
39
40
41
42
43
44
45
46
47
48
49
50

51
52 Given how low the overall protein coverage is in each case, it is interesting that the
53 small amounts of BSA adsorbed make any difference at all, since the incoming fibrinogen
54
55
56
57

1
2
3 might be expected to simply bind in the spaces left by the BSA. However, it is well known
4
5 that in general, adsorption of surfactant molecules may occur preferentially at certain more
6
7 'active' metal surface sites⁴⁴⁻⁴⁶; as the NR technique yields structural information averaged
8
9 in the z-direction, we cannot draw any conclusions concerning the specific locations of the
10
11 SDS/BSA adsorption, but it may be that even a relatively low coverage is sufficient to block
12
13 sites at which fibrinogen preferentially interacts with the stainless steel surface and hence
14
15 inhibit its adsorption.
16
17

18
19 For both samples, a significant amount of protein was left on the surface after
20
21 washing with PBS solutions containing no dissolved protein (Table 2, represented by protein
22
23 concentrations of '0 ppm'), confirming that the adsorption is at least partially irreversible, as
24
25 has been observed for both fibrinogen and BSA on various surfaces previously^{38,47}, and in
26
27 good agreement with the QCM results to be presented below.
28
29

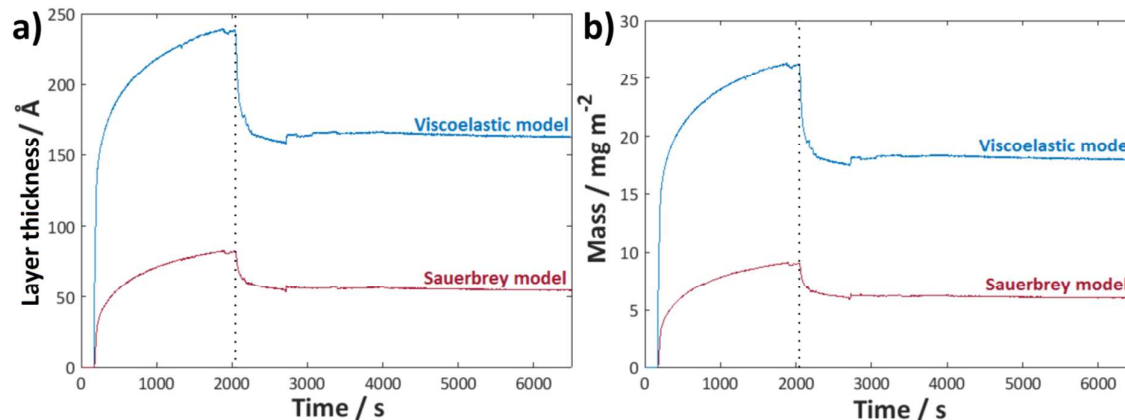
30 QCM.



51
52 **Figure 5. QCM frequency and dissipation data for 316 stainless steel sensor under PBS**
53 **(blue), with 30,000 ppm BSA added (orange) and flushed again with PBS (blue).**
54
55

1
2
3 Figure 5 shows the variation in frequency and dissipation for a 316 stainless steel
4 sample after exposure to 30,000 ppm BSA/PBS, and then following rinsing in PBS, as marked
5 on the plot. It is clear that a significant amount of protein was adsorbed, and that although
6 on the plot. It is clear that a significant amount of protein was adsorbed, and that although
7 the PBS rinse removed roughly a third of this adsorbed protein essentially immediately, the
8 rest was stable over a prolonged period of measurement.
9
10
11
12
13

14 The separation of the frequency measurements for the different fundamentals and
15 the variable dissipation suggest the adsorbed protein cannot be treated as a simple, rigid
16 layer as assumed by the Sauerbrey model, although the layer appears to become more
17 Sauerbrey-like after the rinse, as evidenced by the frequency lines moving closer together. A
18 viscoelastic model gave a reasonable fit to the data (Figure S2) and the adsorbed layer
19 thicknesses and masses predicted by the different models are compared in Figure 6.
20
21
22
23
24
25
26
27
28
29



50
51
52
53
54
55
56
57
58
59
60

Figure 6. Predicted a) layer thicknesses and b) masses resulting from the Sauerbrey and viscoelastic models, as labelled. The reintroduction of PBS is marked with a dotted line.

Interestingly, the adsorbed mass predicted by both models, as shown in Figure 6b is much greater than that calculated from the fit to the neutron data—by well over an order of magnitude in the case of the viscoelastic model. This discrepancy is presumed to arise from

the acknowledged inability of QCM measurements to differentiate between the protein and associated water in less rigid protein films, which may lead to a significant overestimation of surface loading. The large difference between the two techniques seen here may be partly explained by some level of protein unfolding, as water retention is often greater in such a case^{48–50}.

The layer thicknesses shown in Figure 6b are calculated using the predicted masses, sensor chip surface area and protein density, and are hence also subject to overestimation. Additionally, as inferred from the NR data, the surface coverage of adsorbed protein is relatively low and so an average thickness is unlikely to correlate well to the actual adsorbed layer thickness, which is best determined using the NR fit. The QCM data are, however, are useful in comparing relative adsorption, as explained below.

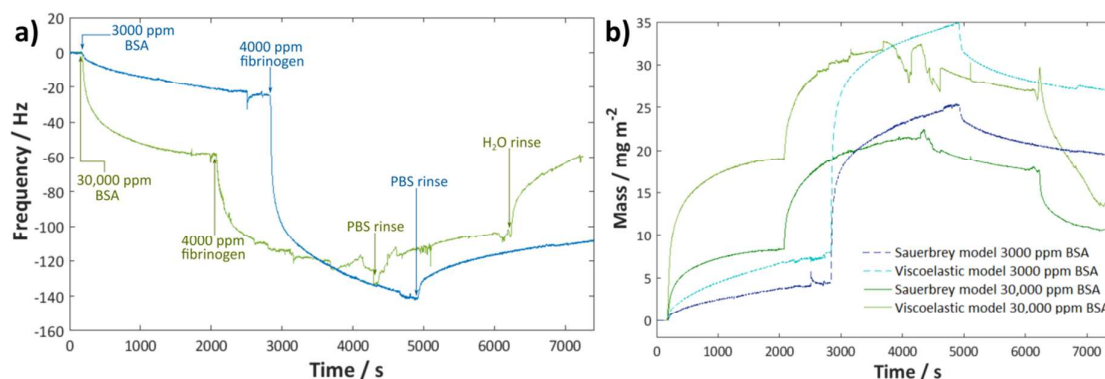


Figure 7a) Comparison of the frequency variation (f_3) with time for the 316 stainless steel chips treated with 3000 (green) or 30,000 ppm (blue) BSA prior to 4000 ppm fibrinogen as labelled. b) Modelled adsorbed masses for these data.

To discern the effects of pre-adsorbed BSA on the subsequent adsorption of fibrinogen, two sensors were treated with 3000 and 30,000 ppm BSA respectively and allowed to equilibrate before 4000 ppm fibrinogen/PBS was exposed to the surface. The results are plotted in Figure 7a, with the adsorbed masses predicted using the

1
2
3 corresponding Sauerbrey and viscoelastic model fits in Figure 7b. It is clear from Figure 7
4
5 that fibrinogen adsorbs to a much lesser extent on the stainless steel surface that has been
6
7 pretreated with the higher concentration of BSA—almost half, in fact (the precise %
8
9 depending on which model type is used to interpret the data). This is in good agreement
10
11 with the model fits derived from the neutron data above, where a significant reduction in
12
13 fibrinogen adsorption was seen when the stainless steel surface was pretreated with BSA. In
14
15 fact, there is an even greater % reduction seen here than for the neutron data, which may
16
17 imply that the fibrinogen adsorbing on the pre-treated surface is less prone to structural
18
19 deformation and hence has less associated water (leading to a lower detected mass).
20
21
22
23
24
25

26 Around a quarter of the adsorbed protein is removed upon rinsing with PBS for both
27
28 samples; this is a little less than was removed for the BSA-only sample above (where around
29
30 a third was removed with a PBS rinse), suggesting the fibrinogen may bond rather more
31
32 strongly to the stainless steel surface. Previous work showed even less protein was removed
33
34 when fibrinogen was adsorbed by itself to a stainless steel surface (around 10%), which
35
36 supports this conclusion²⁵. The neutron data fits above also estimate around 25% protein is
37
38 removed for the BSA-coated sample exposed to fibrinogen (Sample 1), in excellent
39
40 agreement with this data.
41
42
43

44 When the rinsing medium was changed to deionized water (for the low BSA
45
46 concentration only), a greatly increased amount of protein was removed from the surface.
47
48 This is attributed to the negligible ionic strength of the water and hence increased Debye
49
50 screening length such that the adsorbed proteins repel each other and are more likely to
51
52 desorb as a result⁵¹.
53
54
55
56
57
58
59
60

CONCLUSIONS

Neutron reflectometry data for a 316L stainless steel surface exposed to an approximately physiological concentration of BSA have shown low surface coverage of the adsorbed protein (< 20%) at an overall thickness of around 80 Å, comprising 3 or 4 fitted blocks with slightly different hydration values. Isotherm models fitted to the data suggested monolayer adsorption at lower concentrations with possible bilayer or multilayer at higher concentrations. The high level of water retention observed from the QCM may also indicate some level of protein unfolding on the surface; a viscoelastic model was necessary to fit the QCM data, indicating that the adsorbed protein exists as a diffuse, weakly-bound layer, in agreement with the NR data.

When a solution of 30,000 ppm and 4000 ppm fibrinogen was exposed to the surface pre-treated with BSA, there was an increase in the total amount of protein adsorbed, which then increased again for a solution of just fibrinogen to the value expected when fibrinogen is introduced to a non pre-treated stainless steel surface. This suggests fibrinogen is extremely effective at displacing adsorbed BSA, even at low concentrations.

A second sample was first treated with SDS resulting in around 46% coverage of the surfactant on the stainless steel surface. As a result, an increased amount of BSA adsorption was observed and an ensuing decrease in fibrinogen adsorption; clearly, the modification of the surface to render it more conducive to BSA adsorption was successful in inhibiting the fibrinogen adsorption. The dramatic decrease (by half) of fibrinogen adsorption seen in the QCM measurements when BSA pre-treatment was increased from 3000 to 30,000 ppm may imply fibrinogen adsorbing on top of BSA is also less prone to unfolding.

1
2
3 When the surfaces treated with protein solutions were washed in PBS solution, less
4
5 protein could be removed (around 25%) if fibrinogen was present than if only BSA had been
6
7 adsorbed (around a third), further supporting observations that fibrinogen has a greater
8
9 affinity for stainless steel than BSA once it has gained access to the surface. Hence, although
10
11 pre-adsorption of BSA is effective in preventing fibrinogen adsorption, over time fibrinogen
12
13 may still adsorb significantly due to the Vroman effect, unless the BSA is more firmly
14
15 anchored.
16
17

18
19 Increasing hydrophobicity of a stainless steel surface by pre-adsorption of a
20
21 surfactant molecule such as SDS may be an effective method of ensuring improved BSA
22
23 adsorption and hence inhibition of fibrinogen. However, in all systems studied, a significant
24
25 amount of fibrinogen was still adsorbed, suggesting these methods are not by themselves
26
27 fully sufficient in ensuring biocompatibility.
28
29
30

31 32 **Acknowledgements**

33
34 With thanks to Juan Rubio-Lara (Nanoscience, University of Cambridge) for the thin film
35
36 depositions. This work is based on experiments performed at the neutron reflectometer
37
38 AMOR at Swiss spallation neutron source SINQ, Paul Scherrer Institute, Villigen, Switzerland.
39
40
41
42
43

44 **Supporting Information**

45
46 Molar isotherms of fibrinogen and BSA on stainless steel for comparison. QCM raw data
47
48 with viscoelastic model fits plotted to show goodness of fit.
49
50
51
52
53

54 55 **REFERENCES**

- 1
2
3 (1) Gorbet, M. B.; Sefton, M. V. Biomaterial-associated thrombosis: Roles of coagulation
4 factors, complement, platelets and leukocytes. *Biomaterials* **2004**, *25*, 5681-5703.
5
6
- 7 (2) Taubert, A.; Mano, J. F.; Rodríguez-Cabello, J. C. *Biomaterials Surface Science*; Wiley-
8 VCH Verlag GmbH & Co. KGaA: Weinheim, 2013.
9
10
- 11 (3) Sprague, E. A.; Palmaz, J. C. A model system to assess key vascular responses to
12 biomaterials. *J. Endovasc. Ther.* **2005**, *12*, 594-604.
13
14
- 15 (4) Tsai, W.; Grunkemeier, J. M.; Horbett, T. A. Human plasma fibrinogen adsorption and
16 platelet adhesion to polystyrene. *J. Biomed. Mater. Res.* **1999**, *44*, 130-139.
17
18
- 19 (5) Yongli, C.; Xiufang, Z.; Yandao, G.; Nanming, Z.; Tingying, Z.; Xinqi, S. Conformational
20 changes of fibrinogen adsorption onto hydroxyapatite and titanium oxide
21 nanoparticles. *J. Coll. Int. Sci.* **1999**, *214*, 38-45.
22
23
- 24 (6) Ding, Y.-X.; Hlady, V. Competitive adsorption of three human plasma proteins onto
25 sulfhydryl-to-sulfoate gradient surfaces. *Croat. Chem. Acta.* **2011**, *84*, 193-202.
26
27
- 28 (7) Slack, S. M.; Horbett, T. A. Changes in fibrinogen adsorbed to segmented
29 polyurethanes and hydroxyethylmethacrylate-ethylmethacrylate copolymers. *J.*
30 *Biomed. Mater. Res.* **1992**, *26*, 1633-1649.
31
32
- 33 (8) Horbett, T. A.; Cheng, C. M.; Ratner, B. D.; Hoffman, A. S.; Hanson, S. R. The kinetics of
34 baboon fibrinogen adsorption to polymers in vitro and in vivo studies. *J. Biomed.*
35 *Mater. Res.* **1986**, *20*, 739-772.
36
37
- 38 (9) Foster, J. R. In *Albumin structure, function and uses*; Rosenoer, V. M., Oratz, M.,
39 Rothschild, M. A., Eds.; Pergamon Press: Great Britain, 1977.
40
41
- 42 (10) Martins, M. C. L.; Wang, D.; Ji, J.; Feng, L.; Barbosa, M. A. Albumin and fibrinogen
43 adsorption on PU-PHEMA surfaces. *Biomaterials* **2003**, *24*, 2067–2076.
44
45
- 46 (11) Keogh, J. R.; Velandar, F. F.; Eaton, J. W. Albumin-binding surfaces for implantable
47
48
49
50
51
52
53
54
55
56
57

- 1
2
3 devices. *J. Biomed. Mater. Res.* **1992**, *26*, 441-456.
4
5 (12) Mulvihill, J. N.; Faradji, A.; Oberling, F.; Cazenave, J.-P. Surface passivation by human
6
7 albumin of plasmapheresis circuits reduces platelet accumulation and thrombus
8
9 formation. Experimental and clinical studies. *J. Biomed. Mater. Res.* **1990**, *24*, 155–
10
11 163.
12
13
14 (13) Kim, S. W.; Lee, R. G.; Oster, H.; Coleman, D.; Andrade, J. D.; Lentz, D. J.; Olsen, D.
15
16 Platelet adhesion to polymer surfaces. *Trans. Amer. Soc. Artif. Int. Organs* **1974**, *20*,
17
18 449-455.
19
20
21 (14) Kottke-Marchant, K.; Anderson, J. M.; Umemura, Y.; Marchant, R. E. Effect of albumin
22
23 coating on the in vitro blood compatibility of Dacron arterial prostheses. *Biomaterials*
24
25 **1989**, *10*, 147-155.
26
27
28 (15) Amiji, M.; Park, H.; Park, K. Study on the prevention of surface-induced platelet
29
30 activation by albumin coating. *J. Biomater. Sci. Polym. Edn.* **1992**, *3*, 375-388.
31
32
33 (16) Munro, M. S.; Quattrone, A. J.; Ellsworth, S. R.; Kulkarni, P.; Eberhart, R. C. Alkyl
34
35 substituted polymers with enhanced albumin affinity. *Trans. Am. Soc. Artif. Intern.*
36
37 *Organs* **1981**, *27*, 499-503.
38
39
40 (17) Holmberg, M.; Hou, X. Fibrinogen adsorption on blocked surface of albumin. *Coll.*
41
42 *Surf. B.* **2011**, *84*, 71–75.
43
44
45 (18) Wertz, C. F.; Santore, M. M. Effect of surface hydrophobicity on adsorption and
46
47 relaxation kinetics of albumin and fibrinogen: single-species and competitive
48
49 behavior. *Langmuir* **2001**, *17*, 3006-3016.
50
51
52 (19) Roach, P.; Farrar, D.; Perry, C. C. Interpretation of protein adsorption: surface-induced
53
54 conformational changes. *J. Am. Chem. Soc.* **2005**, *127*, 8168-8173.
55
56
57 (20) Uyen, H. M. W.; Schakenraad, J. M.; Sjollem, J.; Noordmans, J.; Jongebloed, W. L.;

- 1
2
3 Stokroos, I.; Busscher, H. J. Amount and surface structure of albumin adsorbed to
4
5 solid substrata with different wettabilities in a parallel plate flow cell. *J. Biomed.*
6
7 *Mater. Res.* **1990**, *24*, 1599–1614.
8
9
10 (21) Hedberg, Y.; Wang, X.; Hedberg, J.; Lundin, M.; Blomberg, E.; Wallinder, I. O. "Surface-
11
12 protein interactions on different stainless steel grades: effects of protein adsorption,
13
14 surface changes and metal release." *J. Mater Sci. Mater. Med.* **2013**, *24*, 1015-1033.
15
16
17 (22) Campana, M.; Hosking, S. L.; Petkov, J. T.; Tucker, I. M.; Webster, J. R. P.; Zorbakhsh,
18
19 A.; Lu, J. R. Adsorption of bovine serum albumin (BSA) at the oil/water interface: a
20
21 neutron reflection study. *Langmuir* **2015**, *31*, 5614-5622.
22
23
24 (23) Penfold, J.; Thomas, R. K. The application of the specular reflection of neutrons to the
25
26 study of surfaces and interfaces. *J. Phys. Condens. Matter* **1990**, *2*, 1369-1412.
27
28
29 (24) Penfold, J.; Thomas, R. K.; Lu, J. R.; Staples, E.; Tucker, I.; Thompson, L. The study of
30
31 surfactant adsorption by specular neutron reflection. *Phys. B.* **1994**, *198*, 110-115.
32
33
34 (25) Wood, M. H.; Browning, K. L.; Barker, R. D.; Clarke, S. M. Using neutron reflectometry
35
36 to discern the structure of fibrinogen adsorption at the stainless steel/aqueous
37
38 interface *J. Phys. Chem. B* **2016**, *120*, 5405-5416.
39
40
41 (26) Voinova, M. V.; Rodahl, M.; Jonson, M.; Kasemo, B. Viscoelastic acoustic response of
42
43 layered polymer films at fluid-solid interfaces: continuum mechanics approach. *Phys.*
44
45 *Scr.* **1999**, *59*, 391.
46
47
48 (27) Björck, M.; Andersson, G. GenX: an extensible X-ray reflectivity refinement program
49
50 utilising differential evolution. *J. Appl. Cryst.* **2007**, *40*, 1174-1178.
51
52
53 (28) Gupta, M.; Gutberlet, T.; Stahn, J.; Keller, P.; Clemens, D. AMOR - the time-of-flight
54
55 neutron reflectometer at SINQ/PSI. *Pramana - J. Phys.* **2004**, *63*, 57-63.
56
57
58 (29) Hughes, A. V. Sourceforge: Downloaded from <http://sourceforge.net/projects/rscl/>
59
60

- 2013.
- (30) Sposito, G. *The Chemistry of Soils*; Oxford University Press: New York, 2008.
- (31) Nakagaki, M.; Handa, T.; Shimabayashi, S. S-shaped adsorption isotherms of surface active electrolytes from aqueous solutions. *J. Coll. Int. Sci.* **1973**, *43*, 521-529.
- (32) Zhu, B.; Gu, T. Surfactant adsorption at solid-liquid interfaces. *Adv. Colloid Interface Sci.* **1991**, *37*, 1-32.
- (33) Squire, P. G.; Moser, P.; O’Konski, C. T. The hydrodynamic properties of bovine serum albumin monomer and dimer. *Biochemistry* **1968**, *7*, 4261-4272.
- (34) Gispert, M. P.; Saramago, B.; Serro, A. P.; Colaço, R. Bovine serum albumin adsorption onto 316L stainless steel and alumina: a comparative study using depletion, protein radiolabeling, quartz crystal microbalance and atomic force microscopy. *Surf. Int. Anal.* **2008**, *40*, 1529–1537.
- (35) Pradier, C. M.; Costa, D.; Rubio, C.; Compère, C.; Marcus, P. Role of salts on BSA adsorption on stainless steel in aqueous solutions. 1. FT-IRRAS and XPS characterisation. *Surf. Int. Anal.* **2002**, *34*, 50–54.
- (36) Singh, M.; Chand, H.; Gupta, K. C. The study of density, apparent molecular volume and viscosity of bovine serum albumin and lysozyme in aqueous and RbI, CsI and DTAB aqueou solutions at 303.15 K. *Chem. Biodivers.* **2005**, *2*, 809-824.
- (37) Fukuzaki, S.; Urano, H.; Nagata, K. Adsorption of protein onto stainless-steel surfaces. *J. Ferment. Bioeng.* **1995**, *80*, 6-11.
- (38) Sakiyama, T.; Tomura, J.; Imamura, K.; Nakanishi, K. Adsorption characteristics of bovine serum albumin and its peptide fragments on a stainless steel surface. *Coll. Surf. B* **2004**, *33*, 77-84.
- (39) Van Enckevort, H. J.; Dass, D. V; Langdon, A. G. The adsorption of bovine serum

- 1
2
3 albumin at the stainless-steel/aqueous solution interface. *J. Coll. Int. Sci.* **1984**, *98*,
4
5 138–143.
6
7 (40) Sheardown, H.; Cornelius, R. M.; Brash, J. L. Measurement of protein adsorption to
8
9 metals using radioiodination methods: a caveat. *Coll. Surf. B* **1997**, *10*, 29–33.
10
11 (41) Hedberg, Y.; Hedberg, J.; Liu, Y.; Wallinder, I. O. Complexation- and ligand-induced
12
13 metal release from 316L particles: Importance of particle size and crystallographic
14
15 structure. *BioMetals* **2011**, *24*, 1099–1114.
16
17 (42) Wertz, C. F.; Santore, M. M. Adsorption and relaxation kinetics of albumin and
18
19 fibrinogen on hydrophobic surfaces: single-species and competitive behavior.
20
21
22
23 *Langmuir* **1999**, *15*, 8884–8894.
24
25 (43) Hedberg, Y. S.; Killian, M. S.; Blomberg, E.; Virtanen, S.; Schmuki, P.; Wallinder, I. O.
26
27 Interaction of bovine serum albumin and lysozyme with stainless steel studied by
28
29 time-of-flight secondary ion mass spectrometry and X-ray photoelectron
30
31 spectroscopy. *Langmuir* **2012**, *28*, 16306–16317.
32
33 (44) Wood, M. H.; Welbourn, R. J. L.; Zorbakhsh, A.; Gutfreund, P.; Clarke, S. M. Polarized
34
35 neutron reflectometry of nickel corrosion inhibitors. *Langmuir* **2015**, *31*, 7062–7072.
36
37 (45) Morales-Gil, P.; Walczak, M. S.; Cottis, R. A.; Romero, J. M.; Lindsay, R. Corrosion
38
39 inhibitor binding in an acidic medium: Interaction of 2-mercaptobenzimidazole with
40
41 carbon-steel in hydrochloric acid. *Corr. Sci.* **2014**, *85*, 109–114.
42
43 (46) Molchan, I. S.; Thompson, G. E.; Lindsay, R.; Skeldon, P.; Likodimos, V.; Romanos, G.
44
45 E.; Falaras, P.; Adamova, G.; Iliev, B.; Schubert, T. J. S. Corrosion behaviour of mild
46
47 steel in 1-alkyl-3-methylimidazolium tricyanomethanide ionic liquids for CO₂ capture
48
49 applications. *RSC Adv.* **2014**, *4*, 5300–5311.
50
51 (47) Chan, B. M. C.; Brash, J. L. Adsorption of fibrinogen on glass: Reversibility aspects. *J.*
52
53
54
55
56
57
58
59
60

1
2
3 *Coll. Int. Sci.* **1981**, *82*, 217-225.
4

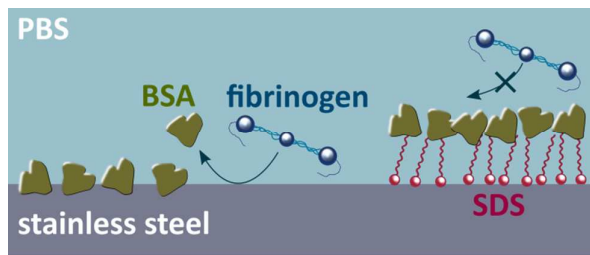
5 (48) Ouberai, M. M.; Xu, K.; Welland, M. E. Effect of the interplay between protein and
6 surface on the properties of adsorbed protein layers. *Biomat.* **2014**, *35*, 6157-6163.
7

8
9 (49) Höök, F.; Kasemo, B.; Nylander, T.; Fant, C.; Sott, K.; Elwing, H. Variations in coupled
10 water, viscoelastic properties and film thickness of a Mefp-1 protein film during
11 adsorption and cross-linking: A quartz crystal microbalance with dissipation
12 monitoring, ellipsometry and surface plasmon resonance study. *Anal. Chem.* **2001**,
13 *73*, 5796-5804.
14
15
16
17
18
19

20
21 (50) Limson, J.; Odunuga, O. O.; Green, H.; Höök, F.; Blatch, G. L. The use of a quartz
22 crystal microbalance with dissipation for the measurement of protein-protein
23 interactions: A qualitative and quantitative analysis of the interactions between
24 molecular chaperones. *S. Afr. J. Sci.* **2004**, *100*, 678-682.
25
26
27
28
29

30 (51) Parkes, M.; Myant, C.; Cann, P. M.; Wong, J. S. S. The effect of buffer solution choice
31 on protein adsorption. *Tribol. Int.* **2014**, *72*, 108-117.
32
33
34
35
36
37
38
39
40
41
42
43
44
45
46
47

48
49 **TOC GRAPHIC**
50
51
52
53
54
55
56
57



1
2
3
4
5
6
7
8
9
10
11
12
13
14
15
16
17
18
19
20
21
22
23
24
25
26
27
28
29
30
31
32
33
34
35
36
37
38
39
40
41
42
43
44
45
46
47
48
49
50
51
52
53
54
55
56
57
58
59
60